Materials Research Express

PAPER • **OPEN ACCESS**

The synergistic effect of biosynthesized silver nanoparticles from a combined extract of parsley, corn silk, and gum arabic: *in vivo* antioxidant, anti-inflammatory and antimicrobial activities

To cite this article: Aya Helmy *et al* 2020 *Mater. Res. Express* **7** 025002

Materials Research Express

PAPER

The synergistic effect of biosynthesized silver nanoparticles from a combined extract of parsley, corn silk, and gum arabic: *in vivo* antioxidant, anti-inflammatory and antimicrobial activities

Aya Helmy[1,8], **Mohamed El-Shazly**[2,3,8], **Amany Seleem**[4], **Usama Abdelmohsen**[5], **M Alaraby Salem**[6], **Ahmed Samir**[6], **Mohamed Rabeh**[1,7,9], **Ali Elshamy**[7] **and Abdel Nasser B Singab**[2,9]

[1] Department of Pharmacognosy, Faculty of Pharmacy, Modern University for Technology and Information (MTI), Cairo, Egypt
[2] Department of Pharmacognosy, Faculty of Pharmacy, Ain-Shams University, Cairo, Egypt
[3] Department of Pharmaceutical Biology, Faculty of Pharmacy and Biotechnology, German University in Cairo, Cairo, Egypt
[4] Department of Pharmacology, National Research Center, Cairo, Egypt
[5] Department of Pharmacognosy, Faculty of Pharmacy, Minia University, Minia, Egypt
[6] Department of Pharmaceutical Chemistry, Faculty of Pharmacy, October University of Modern Sciences and Arts (MSA), Cairo, Egypt
[7] Department of Pharmacognosy, Faculty of Pharmacy, Cairo University, Cairo, Egypt
[8] Authors equally contributed to the work.
[9] Authors to whom any correspondence should be addressed.

E-mail: dean@pharma.asu.edu.eg **and** mohamedabdelatty68@yahoo.com

Keywords: silver nanoparticles, antioxidant, anti-inflammatory, antimicrobial, parsley, corn silk, gum Arabic

OPEN ACCESS

RECEIVED
14 October 2019

REVISED
14 January 2020

ACCEPTED FOR PUBLICATION
21 January 2020

PUBLISHED
4 February 2020

Abstract

Microbial resistance, oxidative stress, and inflammatory conditions are among the leading causes of death worldwide. In the current work, silver nanoparticles (AgNPs) were biosynthesized using the aqueous extracts of parsley, corn silk (CS), gum Arabic (GA) or combination of the three extracts. The formed nanoparticles were characterized using three techniques including transmission electron microscopy (TEM), UV-visible spectrophotometer and Fourier-transform infrared spectroscopy (FTIR). The antioxidant, anti-inflammatory, and antimicrobial activities were tested for the formed nanoparticles, the aqueous extracts of each of the three plants and their combination. Oxidative stress was induced by alloxan which promoted the development of diabetes mellitus in rats. Inflammation was induced by injecting carrageenan in rats' paws. Pathogenic microorganisms causing serious urinary tract infection (UTI) were selected for the antimicrobial assay. All aqueous extracts and the biosynthesized AgNPs showed variable degrees of antioxidant, anti-inflammatory and antimicrobial activities, however, the AgNPs biosynthesized by the combination of the three aqueous extracts was the most effective one. LC/MS was done to identify the compounds present in the crude extracts that may be responsible for the observed biological activities. LC/MS resulted in the identification of 13 compounds. Docking experiments on COX-1 (cyclooxygenase-1) and COX-2 (cyclooxygenase-2) were performed to determine the compounds responsible for the anti-inflammatory activity of the extracts. The results showed that silver nanoparticles synthesized by the combination of the three aqueous extracts are considered promising candidates for the development of antioxidant, anti-inflammatory and antimicrobial agents.

1. Introduction

Nanotechnology is a rapidly expanding field which involves the synthesis and characterization of noble metals such as silver, gold, and platinum as nanoparticles. The importance of nanotechnology relies on its wide applications in drug delivery, bioengineering, textile engineering, biological labeling, biotechnology, catalysis, water treatment and the detection of genetic disorders [1–4]. Nanoparticles are of maximum size of 100 nm showing different chemical, optical, mechanical, electronic and magnetic properties than larger particles due to the variation in specific characteristics such as shape, size and atomic distribution [1, 5]. Many methods are employed for the synthesis of nanomaterials such as heat evaporation [6], chemical reduction [7–9],

photochemical [10], electrochemical [7, 11], reverse micelle [12], thermal decomposition [13], radiation [7, 14] and microwave-assisted [7] methods. Most of these methods require the use of hazardous chemicals and high energy for the preparation of nanoparticles. Biological synthesis of nanoparticles involves the use of natural materials such as plants, bacteria, fungi [1, 5, 15]. The use of plants for the synthesis of nanoparticles have an advantage over other biological methods as it does not involve the use of cell culture, and does not need longer incubation time required for the reduction of metal ions [16, 17]. Plants are known to contain various secondary metabolites such as alkaloids, terpenoids, flavonoids and tannins which provide suitable reducing and surface agents for the nanoparticle synthesis and stabilization. Biopolymers such as cellulose, chitosan, alginate, dextran and tree gums are another family of natural sources which were used for the reduction and stabilization of nanoparticles [17, 18].

Recently, pathogenic bacteria and fungi such as *Staphylococci* spp., *Enterococci* spp., *Klebsiella pneumoniae,* and *Pseudomonas* spp. demonstrated resistance to commercially available antimicrobial agents at an increasing rate and has become a global threat especially in developing countries. To obviate this, nanoparticles were recently used which provide a new strategy for the development of new antimicrobial agents [2, 19–22]. Among noble metals, silver shows disinfecting, antimicrobial properties and tremendous medicinal value [7, 23]. AgNPs show antimicrobial activity by the direct attachment to the cell wall, disturbing cell-wall permeability, and cellular respiration. These nanoparticles penetrate microbial cells causing damage by interacting with DNA and proteins. AgNPs perform this activity without affecting normal cells and does not easily provoke microbial resistance [24]. AgNPs possess strong anti-inflammatory and antioxidant activities. AgNPs showed effective antibacterial efficacy against *Klebsiella pneumoniae*, *Escherichia coli,* and *S. aureus* in previous reports [25–27]. Thus, the green synthesis of spherical AgNPs with potent antimicrobial, anti-inflammatory, and antioxidant properties is an interesting target. These nanoparticles can be utilized in food, cosmetics, biomedical and pharmaceutical industries [28].

Plants were used for the green synthesis of nanoparticles and the developed green protocols demonstrated many advantages over chemical synthesis. Certain plants rich in antioxidants were superior in the green synthesis of biologically active nanoparticles. The use of local plants, plants exudates, and plants waste products for the synthesis of nanoparticles emerged as an interesting methodology for the preparation of biologically active nanoparticles with minimal cost and adverse effects on human beings and environment. Parsley (*Petroselinum crispum*) leaves are a rich source of ascorbic acid which plays a vital role as a strong reducing agent in the synthesis of nanoparticles. AgNPs synthesized from silky hairs of corn (*Stigma maydis*) displayed potent antibacterial activity against foodborne pathogenic bacteria such as *Listeria monocytogenes*, *Bacillus cereus*, *E. coli*, *Staphylococcus aureus* and *Salmonella Typhimurium*, exhibited potent synergistic antibacterial activity with standard antibiotics and anticandidal activity with amphotericin B. In previous reports, the corn silk (CS) AgNPs showed potent antioxidant activity as demonstrated by 2,2-diphenyl-1-picrylhydrazyl (DPPH) radical scavenging, 2,2'-azino-bis(3-ethylbenzothiazoline-6-sulfonic acid (ABTS) radical scavenging, nitric oxide scavenging and reducing power assays [28].

Tree gums were used as a template for the synthesis of various metals and metal oxide nanoparticles due to the presence of polysaccharides which are effective reducing agents. Also, gums are non-toxic and biodegradable materials used for the stabilization of nanoparticles [18, 29]. The use of gum Arabic (GA) for coating of AgNPs stabilizes the nanoparticles against aggregation, which enhance the transportation and toxicity of the synthesized nanoparticles. GA AgNPs are effective antimicrobial agents against *E. coli*, *Pseudomonas aeruginosa* and *Micrococcus luteus* bacteria [30, 31].

The current study focuses on the green synthesis of AgNPs using three different aqueous plant extracts namely; parsley, CS, or GA. We selected these plants because they are locally available, inexpensive and generally used in folk medicine as a combination therapy for the treatment of urinary tract disorders resulting from inflammation, oxidative stress or infection. We compared the effectiveness of each plant extract before and after the synthesis of AgNPs as antimicrobial, anti-inflammatory and antioxidant agents. A combined extract was formulated of the three previously mentioned aqueous extracts to investigate the synergistic effect of the three different extracts. LC/MS was done to identify the possible compounds that may be responsible for the synthesis and stabilization of the AgNPs. Docking experiment was employed on the identified compounds to determine the possible compounds responsible for the anti-inflammatory activity.

2. Materials and methods

2.1. Plant material

Fresh aerials parts of *P. crispum* (parsley), *S. maydis* (CS) and gummy exudate of *Acacia senegal* (GA) were purchased from the local markets, identified and authenticated by Dr Nada Mostafa, Pharmacognosy Department, Faculty of Pharmacy, Ain-Shams University. Voucher samples were deposited at the Herbarium of

Pharmacognosy Department, Faculty of Pharmacy, Ain-Shams University with the numbers: Parsley (PHG-P-PC 198), corn silk (PHG-P-ZM 197) and gum Arabic (PHG-P-AS 199). Parsley herb and CS were carefully washed with tap water followed by distilled water to remove impurities. They were left to dry for several days at room temperature to remove any moisture. GA was sieved to remove any foreign matters. The dried plant parts and the sieved GA were then ground with an electric blender to obtain fine powder that was stored in amber-colored and airtight bottles in the fridge until further use.

2.2. Animals

All animal procedures and care were conducted according to the general guidelines of the Research Ethics Committee of the National Research Center, Cairo, which conformed with the guiding principles of the International Council on Harmonization and the Islamic Organization for Medical Sciences, the United States Office for Human Research Protections and the United States Code of Federal Regulations and operated under Federal Wide Assurance No.FWA00006444.

2.3. Chemicals

All reagents were purchased of analytical grade and used without any further purification. Silver nitrate ($AgNO_3$) $\geqslant$ 99.0% purity, carrageenan, alloxan were purchased from Sigma-Aldrich (Sigma Aldrich, St. Lewis, USA), Indomethacin was purchased from Epico (Epico, Egyptian Int. Pharmaceutical industries Co., Cairo, Egypt), Metformin (Cidophage)® was obtained from Chemical Industries Development (Chemical Industries Development (CID), Giza, Egypt), Vitamin E was obtained from Pharco (Pharco Pharmaceutical Co., Alexandria, Egypt). Distilled water was used for the preparation of the aqueous extracts in all the experiments.

2.4. Biochemical kits

Biodiagnostic kit for the assessment of blood glucose level and Biodiagnostic Glutathione kit for the assessment of the antioxidant activity were supplied by Diamond Diagnostics (Diamond Diagnostics Chemical Company, Cairo, Egypt).

2.5. Microorganisms

Bacterial and yeast cultures used in this study were obtained from the Microbial Type Culture Collection (MTCC) IMTECH, Chandigarh and from the American type culture collection (ATCC). The bacterial strains were *Staphylococcus saprophyticus* (ATCC 15305), *Enterococcus faecalis* (ATCC 29212), *Escherichia coli* (MTCC 443) and *Pseudomonas aeruginosa* (MTCC 1034), and the yeast strains of Candida were *Candida albicans* (MTCC 183, 227) and for Cryptococcus, the used strain was *Cryptococcus neoformans* (RCMB 0049001). These strains were used for the *in vitro* evaluation of the antimicrobial activity. All the tested microorganisms were supplied by the Microbiology Department, Faculty of Sciences, Al-Azhar University.

2.6. Synthesis of silver nanoparticles by the use of aqueous plants' extract

Parsley herb, CS and GA (5 grams) were added to 100 ml distilled water and kept in a water bath at 60 °C for 30 min, except for GA as the water bath time was extended to 60 min to deactivate the oxidase enzyme. The decoction was then filtered through Whatman No.1 filter paper. The filtrate (aqueous extract) was used as a control and for comparison in the characterization and biological studies. The synthesis of silver nanoparticles was done by the addition of different aqueous extracts to 1 mM (0.001 M) silver nitrate in a ratio (2:10) followed by the addition of two drops of 1 N NaOH and kept in a water bath for 10 min at 60 °C.

2.7. Characterization of the biosynthesized AgNPs

Characterization of the biosynthesized AgNPs was done using three techniques: TEM, UV-visible spectrophotometer and FTIR. TEM was performed by the addition of a drop of AgNPs solution on a copper grid, which was coated with carbon-supported film then left to dry under ambient conditions. After 10 min, the shape and size of the synthesized AgNPs were analyzed using TEM (JEOL model JEM-1010EX). The formation of AgNPs was monitored by measuring the UV-visible spectrum of the reaction medium in the wavelength range from 300 to 600 nm using a UV-visible spectrometer (Shimadzu A116351) using distilled water as the reference. FTIR was used to identify the functional groups in the aqueous extracts responsible for the capping and stabilization of AgNPs. We used Shimadzu FTIR-84005 in the wavelength range 4000–500 cm^{-1}.

2.8. Experimental design

2.8.1. Antioxidant activity

The antioxidant activity of parsley, CS or GA aqueous extracts and their biosynthesized AgNPs, as well as the combination formula, were evaluated in terms of the reduced glutathione (GSH) level and compared with that of

vitamin E as the standard [32]. This method is based on the reduction of 5,5'-dithiobis(2-nitrobenzoic acid) (DTNB) with GSH to produce a yellow-colored compound. The reduced chromogen is directly proportional to the GSH concentration and its absorbance can be measured at 405 nm.

$$\text{Calculation of Glutathione conc.: GSH in blood} = A_{sample} * 66.66\ (mg/dl)$$

A_{sample}: absorbance of the sample at 405 nm.

Male albino rats of Sprague Dawley Strain (130–140 g) were kept under the same hygienic conditions and were given an intraperitoneal injection of alloxan (150 mg kg^{-1} body weight) to induce diabetes mellitus [33]. Hyperglycemia was assessed after 72 h by measuring the blood glucose level [34]. Animals were randomly classified into 12 groups and each group contained five animals. The groups were treated according to the following scheme: **Group I:** Normal group that received 1 ml of saline and served as the normal healthy control; **Group II:** Diabetic group that received 1 ml saline and served as the control; **Group III:** Diabetic group that received 1 ml $AgNO_3$ and served as the positive control group; **Group IV:** Diabetic group that received 7.5 mg kg^{-1} body weight of vitamin E; **Groups V-VIII:** Diabetic group that received 200 mg kg^{-1} body weight of the aqueous plant extracts of parsley, CS, GA and combination from the three aqueous extracts, respectively; **Groups IX-XII:** Diabetic group that received 200 mg kg^{-1} body weight of the biosynthesized AgNPs by parsley, CS, GA and combination from the three aqueous extracts, respectively. Data are presented as mean + S.E from five animals in each group. Statistical significance was evaluated using the ANOVA test followed by post hoc Duncan's multiple range test. A probability value of less than 0.05 was considered statistically significant ($P < 0.05$).

2.8.2. Anti-inflammatory activity

The anti-inflammatory effect was determined through the induction of inflammation by sub plantar injection of carrageenan [35].

Fifty-five male albino rats, weighing (130–150 g), were divided into eleven groups, each group of five animals: **Group I:** Rats that received 1 ml of saline and served as the control; **Group II:** Received 1 ml $AgNO_3$ and served as the positive control group; **Groups III-IV:** Rats that received 200 mg kg^{-1} body weight of the aqueous plant extracts of parsley, CS, GA and combination from the three aqueous extracts, respectively; **Group VII-X:** Rats that received 200 mg kg^{-1} body weight of the biosynthesized AgNPs by parsley, CS, GA and combination from the three aqueous extracts, respectively; **Group XI:** Rats that received 20 mg kg^{-1} of the reference drug indomethacin.

One hour later, all the animals received a sub plantar injection of 0.1 ml of 1% carrageenan suspension in saline in the right hind paw. The thickness of the right hind paw (mm) was measured immediately before and 1, 2, 3 and 4 h post carrageenan injection with a micrometer caliper. The results were expressed as mean S.E. (n = 5). The statistical comparison between the control group and the treated groups was carried out using two-way ANOVA followed by Duncan's multiple range test. The results were statistically significant at $P < 0.05$.

$$\%\text{Edema} = \frac{\text{Thickness of the right paw} - \text{Thickness of the left paw}}{\text{Thickness of the left paw}} * 100$$

2.9. Antimicrobial activity

2.9.1. Sensitivity of bacteria and yeast to the prepared extracts

The antimicrobial screening was done by the agar well diffusion method [36, 37]. Twenty milliliters (20 ml) of molten sterile Mueller-Hinton agar was poured into the sterile Petri dishes and allowed to solidify. Bacterial or fungal inoculum containing 5×10^6 CFU/mL suspensions were uniformly streaked on the surface of the agar using sterile cotton swabs. The agar was then punched aseptically using a sterile tip to make a hole 5 mm in diameter. Twenty microliters of the different extracts were added to each well. Three replicates were performed for each treatment and incubated for 18–22 h at 37 °C bacteria and for 24 h at 25 °C for yeasts. At the end of the incubation period, the inhibition zones diameters of all three replicates were measured in millimeters using a measuring slide and the mean of the three measurements was determined. The antimicrobial activity was indicated by a clear zone in the agar, which was measured after treatment. $AgNO_3$ and was used as the control.

2.9.2. Determination of the minimum inhibitory concentration (MIC) of the prepared extracts by micro-dilution method

To characterize the antibacterial activity of the synthesized AgNPs and the aqueous plants' extracts, broth microdilution method was performed according to the Clinical and Laboratory Standards Institute (CLSI) standards using four quality control strains (CLSI, 2015). The set contained two Gram-negative strains: *E. coli* and *P. aeruginosa*, as well as two Gram-positive strains: *Staphylococcus saprophyticus* and *Enterococcus faecalis*. An inoculate of the microbial strains was prepared from the 24 h broth cultures and the suspensions were adjusted

to 0.5 McFarland standard turbidity. Each sample (100 mg) was dissolved in DMSO (1 ml) to obtain 10 000 μg mL^{-1} stock solution. A number of wells were reserved in each plate for the positive and negative controls. Sterile broth (100 μl) was added to the well from row B to H. The stock solutions of the samples (100 μl) were added to the wells in rows A and B. The mixture of the samples and sterile broth (100 μl) in row B was transferred to each well in order to obtain a twofold serial dilution of the stock samples. The inoculums (100 μl) were added to each well and a final volume of 200 µl was obtained in each well. Plates were incubated at 37 °C for 24 h. Experiments were repeated in duplicates and the results were determined as an average value. The MIC endpoint was considered as the lowest concentration of the extract or fraction inhibiting the total growth of the microorganisms. MIC was detected by the lack of visual turbidity (matching the negative growth control).

2.10. Metabolomic profiling of P. crispum, S. maydis and a combination of the three crude extracts

Metabolomic profiling was performed on the crude extracts of *P. crispum*, *S. maydis* and a combination of the three crude extracts to deliver general qualitative and quantitative profiles of metabolites that may be involved in the activity of the extracts [38]. Dereplication refers to the rapid identification of the known secondary metabolites and their quantification in crude unfractionated extracts [39, 40]. Identification of metabolome was done on an Acquity Liquid Chromatography (LC) system coupled to a Synapt G2 HDMS quadrupole time-of-flight hybrid mass spectrometer (Waters, Milford, USA). Chromatographic separation was carried out on a BEH C18 column (2.1 × 100 mm, 1.7 μm particle size; Waters, Milford, USA) with a guard column (2.1 × 5 mm, 1.7 μm particle size) and a linear binary solvent gradient of 0%–100% eluent B over 6 min at a flow rate of 0.3 ml min^{-1}, using 0.1% formic acid in water (v/v) as solvent A and acetonitrile as solvent B. The injection volume was 2 μl and the column temperature was 40 °C. To convert the raw data into separate positive and negative ionization files, Ms converter software was used. The files were then imported to the data mining software MZmine 2.10 for peak picking, deconvolution, deisotoping, alignment, and formula prediction. The database used for the identification of compounds was the Dictionary of Natural Products (DNP) 2015.

2.11. Molecular docking

Docking was done on the ovine COX-1 enzyme complexed with ibuprofen (PDB ID:1EQG) and human COX-2 enzyme complexed with mefenamic acid (PDB ID: 5IKR) to suggest which compounds identified in LC/MS that might be responsible for the anti-inflammatory activity of the crude extracts. In all docking experiments, a grid box of dimensions 50 grid points and spacing 0.375 was centered on the given co-crystallized ligand. A total of 13 molecules were docked with four starting conformations. These conformers were generated for each ligand using OpenBabel [41] and the docking experiments were performed via Autodock4 [42] implementing 100 steps of genetic algorithm while keeping all the default setting provided by Autodock Tools. Visualization was done using Molecular Operating Environment MOE.

3. Results and discussion

3.1. Characterization of the synthesized AgNPs

3.1.1. Characterization using TEM

TEM analysis showed that the mean size ranged between 8.16–13.35 nm for AgNPs prepared by parsley aqueous extract, 5.28–9.39 nm for AgNPs prepared by CS extract and 6.56–21.47 nm for AgNPs prepared by GA aqueous extract (figure 1). TEM suggested that the morphology of the synthesized nanoparticles is spherical with a mean size in the nano range which indicated the synthesis of AgNPs.

3.1.2. Characterization of AgNPs using UV-Visible spectrophotometer

On the addition of different volumes of the aqueous extracts (1, 2, 3, 4 and 5 ml) to a constant concentration of $AgNO_3$ solution (10 ml of 1 mM solution), a preliminary visual observation showed that the initial color of the reaction mixture was faint, then changed from pale-yellow to light brown then to dark brown exponentially with reaction-time (figure 2). Changing the color of the reaction from light to dark brown with the reaction-time as aggregation proceeds confirmed the formation of silver nanoparticles [43].The solutions were analyzed using UV spectra. AgNPs solutions prepared by parsley, CS and GA aqueous extracts showed absorbance peaks at 418, 419 and 422 nm, respectively (figure 3). The absorbance bands were observed at 410–450 nm, which were similar to those reported in the literature. The intensity of the absorption increased with increasing the concentration of different extracts. These changes in the absorbance confirmed the changes in the particles' sizes during nanoparticles synthesis [44–46].

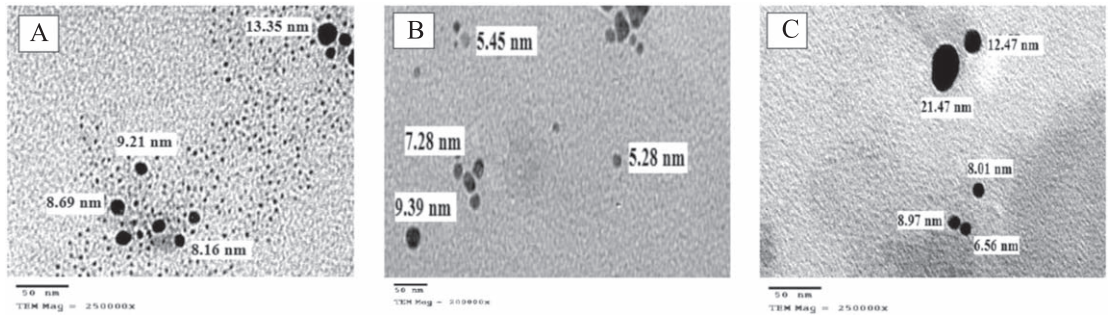

Figure 1. TEM photos for the synthesized AgNPs from the aqueous extracts of *P. crispum* (A), *S. maydis* (B) and GA (C).

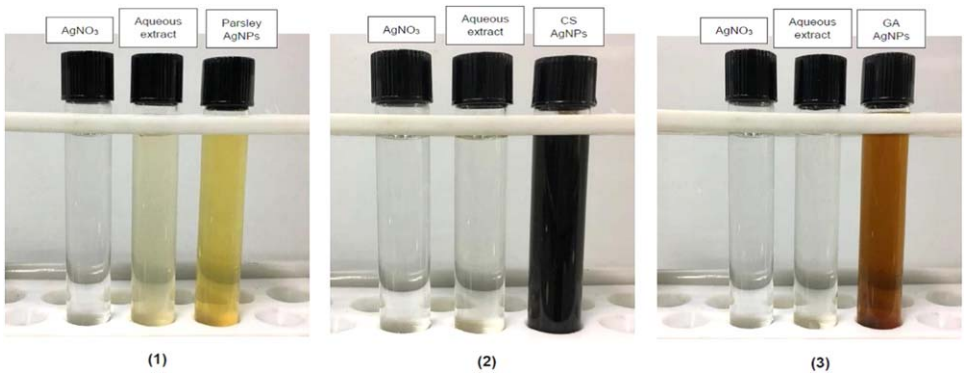

Figure 2. Early signs of AgNPs formation in (1) parsley, (2) CS and (3) GA aqueous extracts observed as the color of the solutions changed to yellowish-brown after 24 h of incubation with 1 mM $AgNO_3$ solution.

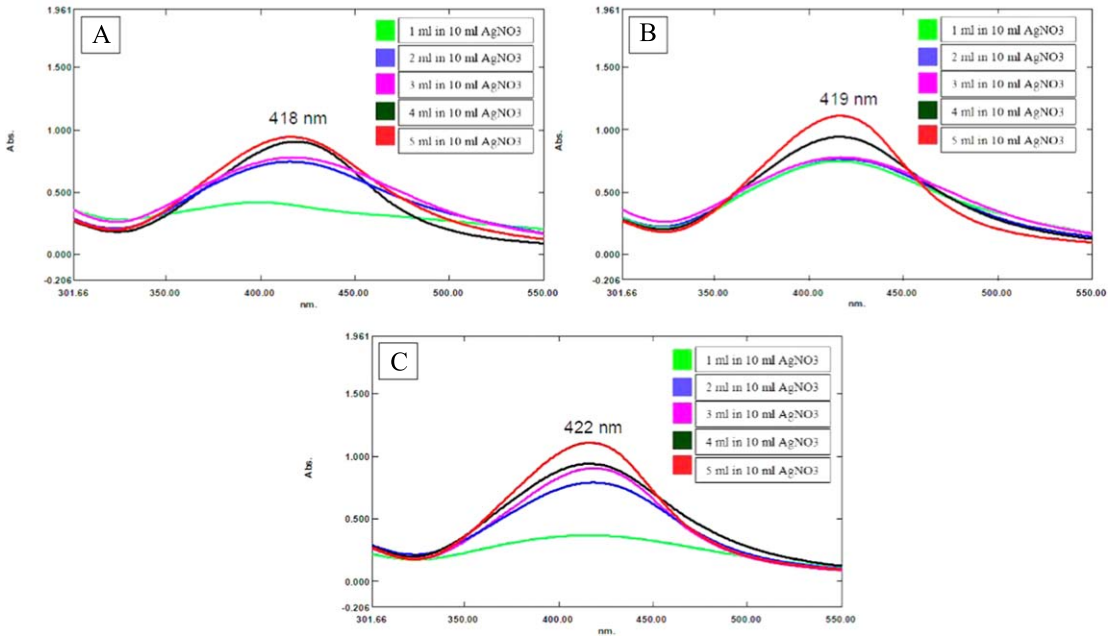

Figure 3. UV-visible spectroscopic analysis of the synthesized AgNPs at five different concentrations of *P. crispum* (A), *S. maydis* (B) and GA (C) solutions.

3.1.3. Characterization of AgNPs using FTIR

FTIR spectra (figure 4) showed major peaks at 3645.46 till 3275.13, 2368.59, 2306.86, 2083.12, 2075.41, 2067.69, 2052.26, 1986.68, 1917.24, 1913.39, 1643.35, 1392.61, 1284.59, 1230.58, 1199.72, 1153.43, 1099.43, 1060.85 and

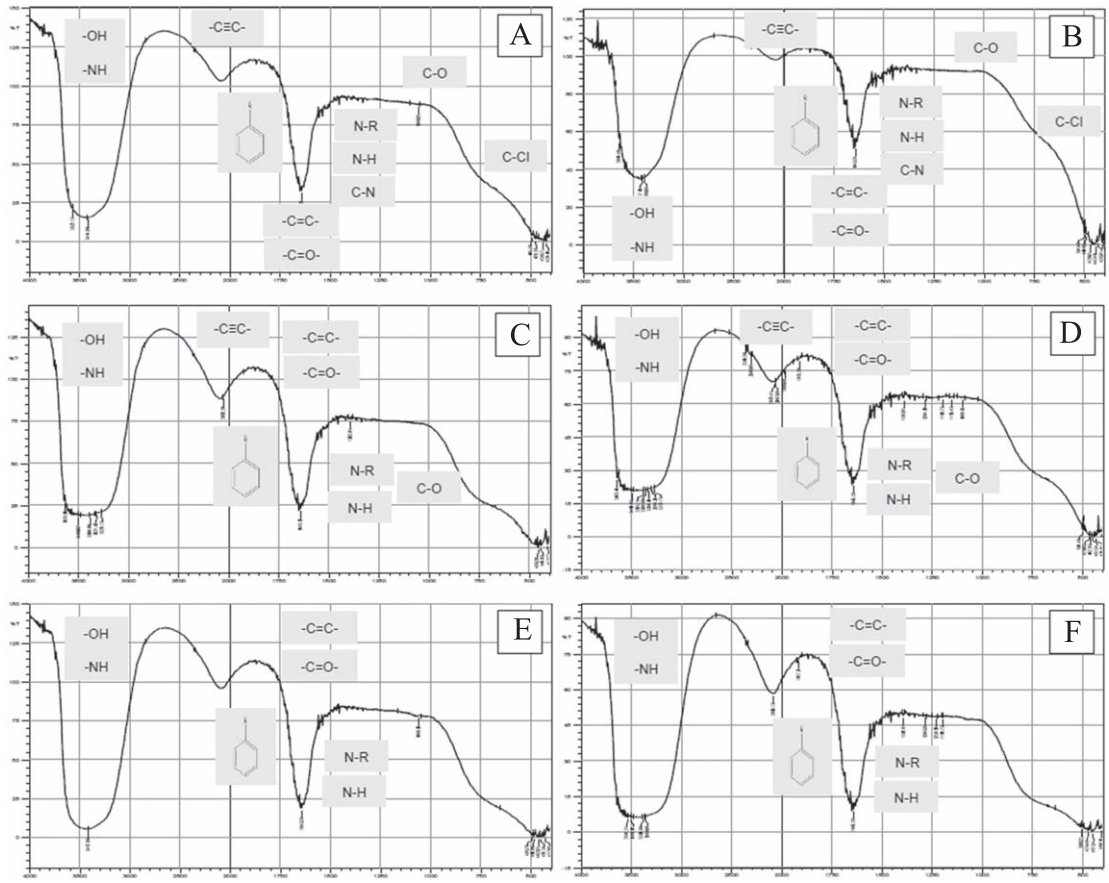

Figure 4. FTRI spectra of *P. crispum* aqueous extract before (A) and after (B) synthesis of AgNPs, *S. maydis* aqueous extract before (C) and after (D) synthesis of AgNPs and GA aqueous extract before (E) and after (F) synthesis of AgNPs.

Table 1. Antioxidant activity of the aqueous extracts of parsley, CS, GA, the combination of the three aqueous extracts, AgNPs synthesized by the three extracts and their combination in male albino rats (n = 5).

Group	Blood glutathione (mg/dl)	% of change from the control
Control	36.7 ± 1.3	—
Diabetic	21.3 ± 0.4*	41.96%
Diabetic + $AgNO_3$	30.4 ± 0.5	17.16%
Diabetic + vitamin E	36.2 ± 1.1	1.36%
Diabetic + Parsley aqueous extract	34.1 ± 0.6	7.08%
Diabetic + CS aqueous extract	32.9 ± 0.5	10.35%
Diabetic + GA aqueous extract	33.6 ± 0.4	8.44%
Diabetic + Combination of the three aqueous extracts	35.1 ± 1.1	4.35%
Diabetic + Parsley AgNPs	34.5 ± 0.9	5.99%
Diabetic + CS AgNPs	33.4 ± 0.7	8.99%
Diabetic + GA AgNPs	34.1 ± 0.8	7.08%
Diabetic + AgNPs prepared a combination of the three aqueous extracts	35.9 ± 0.2	2.17%

*Statistically significant different form control group at $P < 0.05$.

509.21 till 408.91 cm^{-1}. The peaks in the range of 3200–3700 cm^{-1} were assigned as stretching of N-H group and OH stretching in alcohols and phenolic compounds with strong hydrogen bonds. The peaks in the range 2368.59-2052.26 cm^{-1} is relevant to the triple bond stretching. The peaks in the range of 1986.68-1913.39 cm^{-1}

Table 2. Anti-inflammatory activity of the aqueous extracts of parsley, CS, GA, the combination of the three aqueous extracts, AgNPs synthesized by the three extracts and their combination in male albino rats (n = 5). .

Group	Zero Paw diameter (mm)	1 h		2 h		3 h		4 h	
		Paw diameter (mm)	Percentage of edema	Paw diameter (mm)	Percentage of edema	Paw diameter (mm)	Percentage of edema	Paw diameter (mm)	Percentage of edema
Control	3.49 ± 0.07	4.67 ± 0.1*	33.8	4.76 ± 0.2*	36.38	4.81 ± 0.1*	37.8	4.94 ± 0.1*	41.5
$AgNO_3$	3.41 ± 0.04	4.48 ± 0.1*	31.3	4.39 ± 0.1*	28.7	4.33 ± 0.6*	26.9	4.28 ± 0.01*	25.5
Parsley aqueous extract	3.45 ± 0.04	4.28 ± 0.07*	24.05	4.21 ± 0.07*	22.02	4.18 ± 0.06*	21.15	4.14 ± 0.08*	20
Corn silk aqueous extract	3.42 ± 0.04	4.16 ± 0.04*	21.6	4.14 ± 0.1*	21.05	4.11 ± 0.09*	20.17	4.05 ± 0.08*	18.4
GA aqueous extract	3.53 ± 0.06	4.44 ± 0.1*	25.8	4.41 ± 0.13*	24.9	4.35 ± 0.01*	22.9	4.31 ± 0.09*	22.1
Combination of the three aqueous extracts	3.51 ± 0.05	4.23 ± 0.57*	20.51	4.12 ± 0.1*	17.3	4.11 ± 0.08*	17.1	4.05 ± 0.09*	15.38
Parsley AgNPs	3.58 ± 0.07	4.22 ± 0.1*	17.8	4.14 ± 0.1*	15.6	4.06 ± 0.08*	13.4	4.02 ± 0.07*	12.3
Corn silk AgNPs	3.49 ± 0.06	4.08 ± 0.1*	16.9	4.02 ± 0.1*	15.1	3.95 ± 0.6*	13.2	3.9 ± 0.4*	11.7
GA AgNPs	3.47 ± 0.08	4.03 ± 0.09*	16.1	3.98 ± 0.06*	14.7	3.91 ± 0.01*	12.7	3.86 ± 0.01*	11.2
AgNPs prepared by the combination of the three aqueous extracts	3.54 ± 0.08	4.06 ± 0.1*	14.68	4.03 ± 0.1*	13.8	3.93 ± 0.08*	11.01	3.87 ± 0.07*	9.3
Indomethacin	3.48 ± 0.08	3.96 ± 0.09*	13.79	3.90 ± 0.06*	12.06	3.85 ± 0.01*	10.6	3.76 ± 0.01*	8.04

*Significantly different from zero time at $P < 0.05$.

Table 3. Antimicrobial activity as indicated by the growth-inhibition zone (mm) of different extracts against different strains of fungi and bacteria against standard antimicrobial agents.

Sample Microorganisms	$AgNO_3$ (C)	Parsley AgNPs	Parsley aqueous extract	GA AgNPs	GA aqueous extract	CS AgNPs	CS aqueous extract	Comb. aqueous extract	Comb. AgNPs	Standard antimicrobial agents
Gram Positive bacteria:										Ciprofloxacin
Staphylococcus saprophyticus	NA	13	NA	18	NA	19	13	NA	19	26 + 0.11
Enterococcus faecalis	NA	17	14	19	NA	14	16	13	19	29 + 0.22
Gram negative bacteria:										Ciprofloxacin
Escherichia coli	NA	18	13	17	12	18	NA	14	22	27 ± 0.12
Pseudomonas aeruginosa	NA	19	14	14	14	18	NA	13	19	31 ± 0.89
Fungi:										Amphotericin B
Candida albicans	NA	16	NA	19	NA	15	NA	NA	18	20.7 + 0.22
Cryptococcus neoformans	NA	NA	NA	14	NA	NA	NA	NA	17	21 + 0.14

Abbreviations: (C), Control; Comb., Combination formula; NA, No activity.

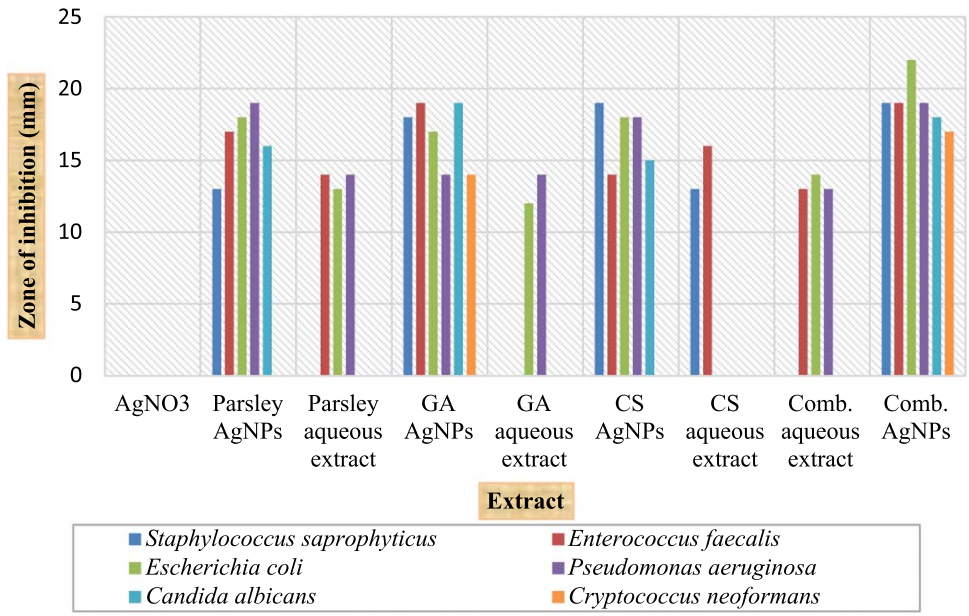

Figure 5. Graphical representation for the antimicrobial activity of different extracts against different strains of fungi and bacteria as indicated by the growth-inhibition zone (mm).

indicated C-H bending of aromatic compounds. The peaks in the range of 1643.35 cm^{-1} indicated C=O bond of the carbonyl group, C=C bond stretching and the stretching vibrations of amides. The peak in the range 1392.61 cm^{-1} indicated the presence of tertiary amide, C-N stretching and N-H bending. Peaks appeared in the range 1284.59-1060.85 cm^{-1} is relevant to C-O stretching, while the peaks in the range 509.21-408.91 cm^{-1} suggested alkyl halides bond stretching.

There are many functional groups present in the aqueous extract of the tested plants which may have been responsible for the reduction of Ag^{+} ions. FTIR spectrum illustrated different peaks positions which were attributed to flavonoids, glycosides, terpenoids, tannins, and phenolics. The presence of such functional groups increased the stability of the synthesized nanoparticles by preventing the clotting and aggregation of the nanoparticles. The similarities between the spectra, before and after synthesis of nanoparticles, with some marginal shifts in peak positions indicated the presence of residuals from the different plant extracts in the sample which acted as a capping agent to the synthesized AgNPs [44, 47]. Therefore, it can be concluded that these secondary metabolites are responsible for the effective stabilization and capping of the synthesized nanoparticles.

3.2. Antioxidant activity

The assessment of GSH level showed that AgNPs prepared by the combination of the three extracts showed the highest antioxidant activity with the change percentage (2.17%), followed by solution of the combined three aqueous with the change percentage (4.35%) and AgNPs prepared by aqueous extract of parsley with the change percentage (5.99%), while the CS aqueous extract showed the least antioxidant activity with change percentage of 10.35% in comparison with Vitamin E as the standard drug with change percentage (1.36%) shown in (table 1). From this table, we can conclude that the antioxidant activity of AgNPs synthesized by the three different aqueous extracts has the highest blood GSH, suggesting the possible synergistic activity of the AgNPs synthesized by the three aqueous plant extracts.

3.3. Anti-inflammatory activity

The anti-inflammatory activity of AgNPs prepared by the combination of the three aqueous extracts was the highest as demonstrated by a time-dependent reduction in edema. The edema was reduced by 14.7%, 13.8%, 11.01%, 9.3% after 1, 2, 3 and 4 h, respectively. GA AgNPs was also active in reducing edema showing 16.1%, 14.7%, 12.7%, and 11.2%, respectively. The GA aqueous extract showed the least anti-inflammatory activity after 1, 2, 3 and 4 h with the following reduction percentages in edema 25.8%, 24.9%, 22.9%, and 22.1%, respectively (table 2). AgNPs synthesized by the three different aqueous extracts showed potent anti-inflammatory activity after four hours resulting in edema reduction suggesting the optimum use of this combination formula as an anti-inflammatory agent. This effect was further confirmed by the aid of the docking technique on two of the well-known enzymes involved in the inflammatory cascade, COX-1, and COX-2.

Table 4. MIC (mg/ml) values of the samples against the tested microorganisms were performed for the most active samples.

Sample Microorganisms	Parsley AgNPs	Parsley aqueous extract	GA AgNPs	GA aqueous extract	CS AgNPs	CS aqueous extract	Comb. aqueous extract	Comb. AgNPs
Gram Positive bacteria:								
Staphylococcus saprophyticus	ND	—	25	—	ND	—	—	100
Enterococcus faecalis	50	ND	25	—	25	ND	ND	25
Gram negative bacteria:								
Escherichia coli	50	100	50	100	50	—	ND	ND
Pseudomonas aeruginosa	50	ND	50	ND	100	—	ND	50
Fungi:								
Candida albicans	ND	—	ND	—	50	—	—	50
Cryptococcus neoformans	—	—	50	—	—	—	—	100

Abbreviations: Comb., combination; ND, not detected.

Table 5. Dereplication of the metabolomics of the crude extracts of *P. crispum*, *S. maydis* and the combined extract formulated from *P. crispum* and *S. maydis* and GA aqueous extracts assembled according to their molecular weight.

m/z	Rt. (min.)	M.wt.	Name	Source	Molecular formula	References
195.15	3.1	194.1423587	Ferulic acid	Corn silk	$C_{10}H_{10}O_4$	[48]
271.061	3.7	270.0533351	Imperatorin	Parsley	$C_{16}H_{14}O_4$	[49]
277.148	1.8	276.1405506	Muurolene dihydrochloride	Parsley Corn silk Combination	$C_{15}H_{26}C_{l2}$	[50]
295.227	4.8	294.2200031	13-Hydroxy-10-oxo-11-octadecenoic acid; (±)-(E)-form, Lactone	Corn silk	$C_{18}H_{30}O_3$	[51]
326.187	4.8	327.1942075	Sophazrine	Corn silk Parsley Combination	$C_{19}H_{25}N_3O_2$	[52]
329.233	3.9	330.2402922	9,18-Dihydroxy-10-octadecenoic acid; (9ξ,10E)-form	Parsley Combination	$C_{18}H_{34}O_5$	[53]
329.233	3.9	330.2402922	5,8,12-Trihydroxy-9-octadecenoic acid	Corn silk Combination	$C_{18}H_{34}O_5$	[54]
338.212	6.4	337.2049716	Holadienine; 18-Oxo, 14,15-didehydro	Parsley	$C_{22}H_{27}NO_2$	[55]
340.202	5.1	341.2094539	Iboluteine; Oxime	Corn silk Parsley Combination	$C_{20}H_{27}N_3O_2$	[56, 57]
356.259	4.3	355.2514057	20-Amino-18-hydroxypregna-1,4-dien-3-one; (20 S)-form, 18-Aldehyde, N,N-di-Me	Corn silk	$C_{23}H_{33}NO_2$	[58]
431.134	3.8	430.1267871	Alternanthin	Corn silk	$C_{22}H_{22}O_9$	[59]
441.322	6.4	440.3139993	8,13-Epoxy-14,15,16,19-labdanetetrol; (ent-8α,13 R,14 S)-form, 19-(3-Methylbutanoyl)	Parsley	$C_{25}H_{44}O_6$	[60]
469.134	2.8	470.141348	4-Hydroxy-5-methyl-2H-1-benzopyran-2-one; O-[β-D-Apiofuranosyl-(1 → 6)-β-D-glucopyranoside]	Parsley	$C_{21}H_{26}O_{12}$	[61]

Abbreviations: Rt, Retention time (min.); M.wt., Molecular weight.

Table 6. The docking scores of the top 10 ligands in Kcal/mol, as generated by Autodock4.

Ligand	COX-1	COX-2
Cocrystallized ibuprofen	−7.1	
Cocrystallized mefenamic acid		−7.4
20-Amino-18-hydroxypregna-1,4-dien-3-one; (20 S)-form, 18-Aldehyde, N,N-di-Me	−11.1	−7.1
Holadienine; 18-Oxo, 14,15-didehydro	−10.7	−8.7
8,13-Epoxy-14,15,16,19-labdanetetrol; (ent-8α,13 R,14 S)-form, 19-(3-Methylbutanoyl)	−10.6	−8.3
Iboluteine; Oxime	−10.1	−7.2
4-Hydroxy-5-methyl-2H-1-benzopyran-2-one; O-[β-D-Apiofuranosyl-(1 → 6)-β-D-glucopyranoside]	−9.9	−10.3
Imperatorin	−9.7	−9.3
13-Hydroxy-10-oxo-11-octadecenoic acid; (±)-(E)-form, Lactone	−9.6	−9.0
Sophazrine	−9.4	−6.3
Muurolene dihydrochloride	−9.4	−8.3
Alternanthin	−9.4	−7.8

*Results are assembled according to their docking scores.

3.4. Antimicrobial activity

3.4.1. Sensitivity of bacteria to the prepared extracts and AgNPs

The antibacterial activity was studied against *S. saprophyticus*, *E. faecalis*, *E. coli* and *P. aeruginosa*. The results indicated that some extracts were active against Gram-positive and Gram-negative bacteria involved in the study (table 3 and figure 5). In case of *S. saprophyticus*, both CS AgNPs and AgNPs prepared by the combination of the three aqueous extracts showed the most potent activity with inhibition zones of 19 mm for both, followed by GA AgNPs with inhibition zone of 18 mm, while all aqueous extracts, except of CS, did not show any activity against the tested microorganisms. For *E. faecalis*, the highest antibacterial activity was seen with GA AgNPs and AgNPs prepared by the combination of the three aqueous extracts with inhibition zones of 19 mm for both, while the

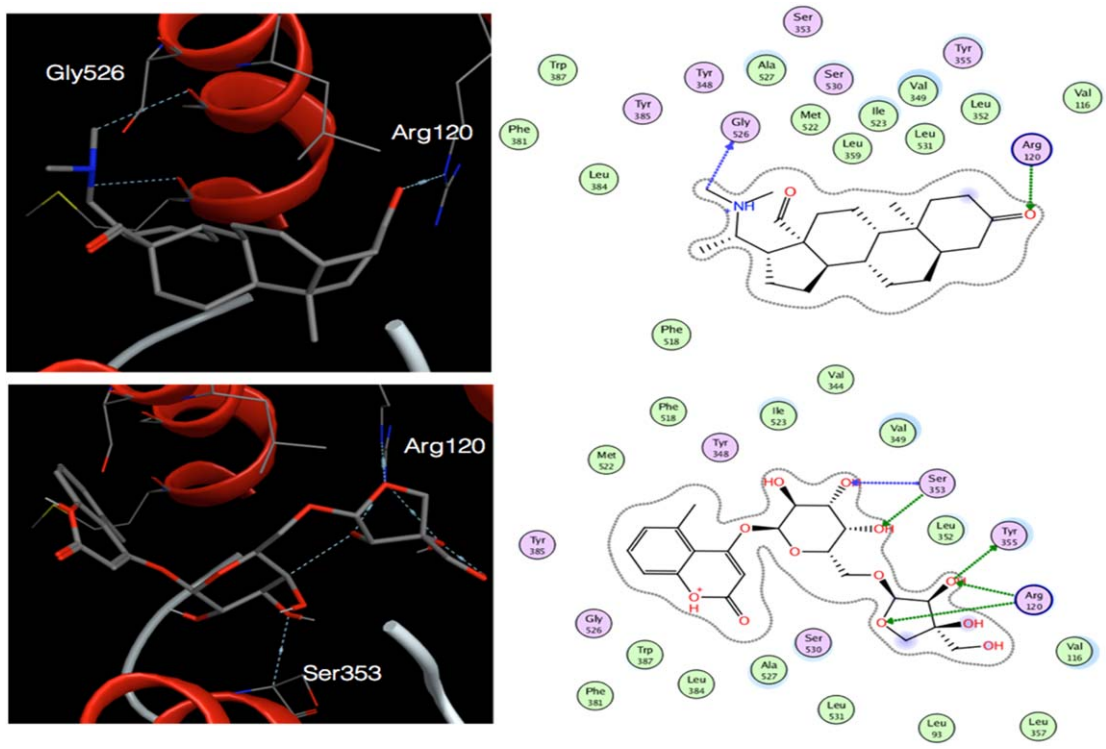

Figure 6. Interaction patterns of 20-amino-18-hydroxypregna-1,4-dien-3-one (top) and 4-hydroxy-5-methyl-2H-1-benzopyran-2-one (bottom).

least antibacterial activity was seen with the combination of the three aqueous extracts with inhibition zone of 13 mm and no activity was seen with GA aqueous extract. AgNPs prepared by the combination of the three aqueous extracts showed the highest inhibitory activity against *E. coli* with inhibition zone of 22 mm followed by parsley AgNPs and CS AgNPs with inhibition zones of 18 mm for both, while the least inhibitory activity was seen with GA aqueous extract with inhibition zone of 12 mm and no activity was detected with CS aqueous extract. For *P. aeruginosa*, AgNPs prepared by the combination of the three aqueous extracts, parsley AgNPs and CS AgNPs showed the highest inhibitory activity with inhibition zones of 19, 19 and 18 mm respectively, while the combination of the three aqueous extracts showed the least inhibitory activity with inhibition zone of 13 mm with no activity was detected for CS aqueous extract.

3.4.2. Sensitivity of yeast to the prepared extracts and AgNPs

The antifungal activity was studied against *C. albicans* and *C. neoformans* (table 3 and figure 5). In case of *C. albicans*, all the synthesized AgNPs showed inhibitory activity with GA AgNPS and AgNPs prepared by the combination of the three aqueous extracts showing the highest activity with inhibition zones of 19 and 18 mm, respectively. All aqueous extracts did not show any activity. For *C. neoformans*, only the AgNPs prepared by the combination of the three aqueous extracts and GA AgNPs showed inhibitory activity without any activity from the aqueous extracts with inhibition zones of 17 and 14 mm, respectively.

From table 3 and figure 5, we can conclude that AgNPs biosynthesized by the three different aqueous extracts showed a broad-spectrum activity against both bacteria and fungi involved in the study, followed by GA AgNPs which also showed inhibitory activity against both bacteria and fungi. These results suggested the possible use of the combination formula as a broad-spectrum antimicrobial agent.

3.4.3. Minimum inhibitory concentration (MIC) of the prepared extracts by microdilution method

The microdilution method, standardized by the Clinical and Laboratory Standards Institute (formerly NCCLS) allowed the determination of the minimal inhibitory concentrations (MICs) of the prepared extracts alone. MIC was determined for some extracts that showed obvious inhibitory activity against the tested microorganisms (table 4).

3.5. Metabolomic profiling of the aqueous extracts of parsley, CS and combined extract of parsley, CS and GA

Dereplication of the secondary metabolites of the aqueous extracts of parsley, CS and the combination formulated from parsley, CS and GA aqueous extracts resulted in the identification of different classes of

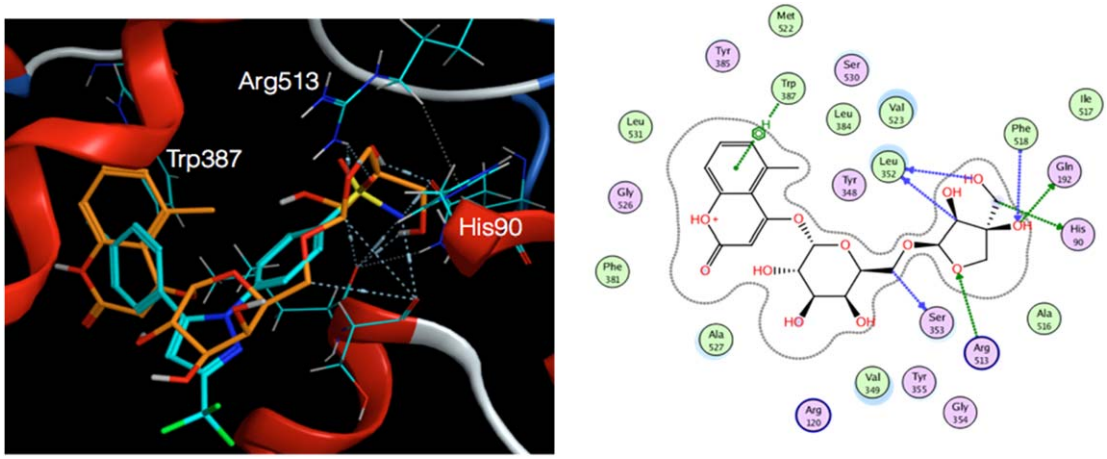

Figure 7. The predicted docked pose of 4-hydroxy-5-methyl-2H-1-benzopyran-2-one in the active site of COX-2 enzyme (orange) and the active conformer of celecoxib (cyan).

compounds. The positive mode showed the majority of the identified compounds and revealed the presence of a variety of alkaloids, terpenes, flavonoids, furanocoumarins, polyphenolic and steroidal compounds (table 5). These identified compounds are responsible for the capping and stabilization of the synthesized AgNPs and might be responsible for the synergistic activity seen in the combination formula.

3.6. Molecular docking

Docking was performed in an attempt to rationalize the observed anti-inflammatory activity of the crude extracts. The top-scoring 10 ligands (according to docking in COX-1) are listed with their docking scores in (table 6).

Most of the compounds identified in the LC/MS spectra showed better or similar scores to the co-crystallized ligands. The scores were significantly better in case of COX-1. According to the scores, the ligands were expected to have more affinity towards COX-1 than COX-2, with the exception of 4-hydroxy-5-methyl-2H-1-benzopyran-2-one; O-[β-D-apiofuranosyl-(1 $\rightarrow$ 6)-β-D-glucopyranoside]. The interactions between the two high-scoring compounds and the surrounding amino acids in the COX-1 active sites are shown in figure 6. Both ligands are expected to form H-bonds with Arg120 in addition to one extra H-bond. The differences between COX-1 and COX-2 active sites are well-studied in literature [62]. It is now common knowledge that COX-2 has an extra binding site that is not present in COX-1. Interactions with Arg513 in COX-2 are also thought to be essential for the selective inhibition of COX-2.41 Interestingly, some of our studied compounds showed excellent binding which was very similar to the known selective COX-2 inhibitors. Figure 7 illustrates how 4-hydroxy-5-methyl-2H-1-benzopyran-2-one; O-[β-D-apiofuranosyl-(1 $\rightarrow$ 6)-β-D-glucopyranoside] assumes a binding conformer that is very similar to that of celecoxib (from the crystal structure 3LN1). As clearly illustrated in the 2D diagram, 4-hydroxy-5-methyl-2H-1-benzopyran-2-one; O-[β-D-apiofuranosyl-(1 $\rightarrow$ 6)-β-D-glucopyranoside] makes many H-bonds including the crucial one with Arg513.

4. Conclusion

The synthesis of AgNPs from aqueous extracts of parsley, CS and GA and combination thereof provided nanoparticles with potent antioxidant, anti-inflammatory, and antimicrobial activity. AgNPs formed by the combined three plants aqueous extracts showed the most potent activity. LC/MS served to identify various compounds that were responsible for the capping and stabilization of the synthesized AgNPs. The docking study pointed out the justification of the anti-inflammatory activity of various extracts in terms of binding to COX-1 and COX-2 enzymes. These findings presented the AgNPs synthesized by the combined extracts of parsley, CS and GA as effective formula for reversing oxidative stress, treatment of various inflammatory conditions and as antimicrobial agents against pathogenic bacteria and fungi causing serious urinary tract infections.

Acknowledgments

The authors are gratefully acknowledged for Maria Lesch (Julius-von-Sachs-Institute of Biosciences, Biocenter, Pharmaceutical Biology, University of Würzburg, Germany) for her help in LC/MS analysis.

Disclosure

The author reports no conflicts of interest in this work.

ORCID iDs

Aya Helmy https://orcid.org/0000-0002-6375-1341

References

[1] Shawkey A M, Rabeh M A, Abdulall A K and Abdellatif A O 2013 Green nanotechnology: anticancer activity of silver nanoparticles using *Citrullus colocynthis* aqueous extracts *Advances in Life Science and Technology* **13** 60–70 (https://pdfs.semanticscholar.org/ff63/48a0de74234df30702a0c6b197b45dd)

[2] Padalia H, Moteriya P and Chanda S 2015 Green synthesis of silver nanoparticles from marigold flower and its synergistic antimicrobial potential *Arabian J. Chem.* **8** 732–41

[3] Almontasser A, Parveen A and Azam A 2019 Synthesis, characterization and antibacterial activity of magnesium oxide (MgO) nanoparticles *In IOP Conference Series: Materials Science and Engineering* **577** 012051

[4] Amal M I, Wibowo J T, Nuraini L, Senopati G, Hasbi M Y and Priyotomo G 2019 Antibacterial activity of copper oxide nanoparticles prepared by mechanical milling *In IOP Conference Series: Materials Science and Engineering* **578** 012039

[5] Mollick M M R *et al* 2015 Studies on green synthesized silver nanoparticles using *Abelmoschus esculentus* (L.) pulp extract having anticancer (*in vitro*) and antimicrobial applications *Arabian J. Chem.* **12** 2572–84

[6] Bae C H, Nam S H and Park S M 2002 Formation of silver nanoparticles by laser ablation of a silver target in NaCl solution *Appl. Surf. Sci.* **197** 628–34

[7] Sharma V K, Yngard R A and Lin Y 2009 Silver nanoparticles: green synthesis and their antimicrobial activities *Adv. Colloid Interface Sci.* **145** 83–96

[8] Panáček A, Kvitek L, Prucek R, Kolář M, Večeřová R, Pizúrová N and Zbořil R 2006 Silver colloid nanoparticles: synthesis, characterization, and their antibacterial activity *The Journal of Physical Chemistry B* **110** 16248–53

[9] Maity D, Kanti Bain M, Bhowmick B, Sarkar J, Saha S, Acharya K and Chattopadhyay D 2011 *In situ* synthesis, characterization, and antimicrobial activity of silver nanoparticles using water soluble polymer *J. Appl. Polym. Sci.* **122** 2189–96

[10] Callegari A, Tonti D and Chergui M 2003 Photochemically grown silver nanoparticles with wavelength-controlled size and shape *Nano Lett.* **3** 1565–8

[11] Yin B, Ma H, Wang S and Chen S 2003 Electrochemical synthesis of silver nanoparticles under protection of poly (N-vinylpyrrolidone) *The Journal of Physical Chemistry* B **107** 8898–904

[12] Lim K T, Hwang H S, Ryoo W and Johnston K P 2004 Synthesis of TiO_2 nanoparticles utilizing hydrated reverse micelles in CO_2 *Langmuir* **20** 2466–71

[13] Jen-La Plante I, Zeid T W, Yang P and Mokari T 2010 Synthesis of metal sulfide nanomaterials via thermal decomposition of single-source precursors *J. Mater. Chem.* **20** 6612–7

[14] Dimitrijevic N M, Bartels D M, Jonah C D, Takahashi K and Rajh T 2001 Radiolytically induced formation and optical absorption spectra of colloidal silver nanoparticles in supercritical ethane *The Journal of Physical Chemistry B* **105** 954–9

[15] Donda M R, Kudle K R, Alwala J, Miryala A, Sreedhar B and Rudra M P 2013 Synthesis of silver nanoparticles using extracts of *Securinega leucopyrus* and evaluation of its antibacterial activity *Int J Curr Sci* **7** E1–8 (http://currentsciencejournal.info/issuespdf/Pratabrudra.pdf)

[16] Satyavani K, Ramanathan T and Gurudeeban S 2011 Green synthesis of silver nanoparticles by using stem derived callus extract of bitter apple (*Citrullus colocynthis*) *Dig J Nanomater Biostruct* **6** 1019–24

[17] Rath M, Panda S S and Dhal N K 2014 Synthesis of silver nano particles from plant extract and its application in cancer treatment: a review *Int J Plant Anim Environ Sci* **4** 137–45 (https://researchgate.net/publication/275337491_Synthesis_of_Silver_nanopart)

[18] Padil V V T, Wacławek S and Černík M 2016 Green synthesis: nanoparticles and nanofibres based on tree gums for environmental applications *Ecol. Chem. Eng.* S **23** 533–57

[19] Paulo C S, Vidal M and Ferreira L S 2010 Antifungal nanoparticles and surfaces *Biomacromolecules* **11** 2810–7

[20] Dheeb B I, Al-dujayli S M, Ibrahim I M, Abbas Q A, Ali A H, Ramizy A and Hussain A F 2019 Study the antifungal activity of ZnS: Mn nanoparticles against some isolated pathogenic fungi *In Journal of Physics: Conference Series* **1178** 012008

[21] Xing Y, Zhu H, Chang G, Yu M, Zhao M and Yue F 2019 Anatase TiO_2 nanoparticles sensitized with organic dyes as efficient antibacterial agents *In IOP Conference Series: Earth and Environmental Science* **252** 022057

[22] Bhattacharya P, Swain S, Giri L and Neogi S 2019 Fabrication of magnesium oxide nanoparticles by solvent alteration and its bactericidal applications *Journal of Materials Chemistry* B **7** 4141–52

[23] Deyá C and Bellotti N 2017 Biosynthesized silver nanoparticles to control fungal infections in indoor environments *Adv. Nat. Sci.: Nanosci. Nanotechnol.* **8** 025005

[24] Ravi D, Sathish S, Parthasarathy R, Priyadharshini M and Revathy M 2013 Synthesis and characterization of silver nanoparticles from *Andrographis paniculata* (Linn.) and it's cytotoxicity against sheep's bone marrow cells *International Journal of Biological & Pharmaceutical Research* **4** 1222–8 (http://ijbpr.com/abstract/Mzgxa2FsYWk=)

[25] Roy K, Sarkar C and Ghosh C 2015 Plant-mediated synthesis of silver nanoparticles using parsley (*Petroselinum crispum*) leaf extract: spectral analysis of the particles and antibacterial study *Applied Nanoscience* **5** 945–51

[26] Bhattacharya P and Neogi S 2017 Gentamicin coated iron oxide nanoparticles as novel antibacterial agents *Mater. Res. Express* **4** 095005

[27] Li P, Li J, Wu C, Wu Q and Li J 2005 Synergistic antibacterial effects of β-lactam antibiotic combined with silver nanoparticles *Nanotechnology* **16** 1912–7

[28] Patra J K and Baek K-H 2016 Biosynthesis of silver nanoparticles using aqueous extract of silky hairs of corn and investigation of its antibacterial and anticandidal synergistic activity and antioxidant potential *IET Nanobiotechnol.* **10** 326–33

[29] Li Y-F, Gan W-P, Jian Z, Lu Z-Q, Chao Y and Ge T-T 2015 Hydrothermal synthesis of silver nanoparticles in Arabic gum aqueous solutions *Transactions of Nonferrous Metals Society of China* **25** 2081–6

[30] Venkatesham M, Ayodhya D, Madhusudhan A and Veerabhadram G 2012 Synthesis of stable silver nanoparticles using gum acacia as reducing and stabilizing agent and study of its microbial properties: A novel green approach *International Journal of Green Nanotechnology* **4** 199–206
[31] Ansari M A, Khan H M, Khan A A, Cameotra S S, Saquib Q and Musarrat J 2014 Gum arabic capped-silver nanoparticles inhibit biofilm formation by multi-drug resistant strains of Pseudomonas aeruginosa *Journal of basic microbiology* **54** 688–99
[32] Beutler E, Duron O and Kelly B 1963 Improved method for the determination of blood glutathione *J. Lab. Clin. Med.* **61** 882–8 (http://garfield.library.upenn.edu/classics1986/A1986A563500001.pdf)
[33] Shabana M, El-Sherei M, Moussa M, Sleem A and Abdallah H 2007 Investigation of phenolic constituents of *Carduncellus eriocephalus Boiss*. var. albiflora Gauba and their biological activities *Natural Product Communications* **2** 823–8
[34] Rather S, Sarumathi A, Anbu S and Saravanan N 2013 Gallic acid protects against immobilization stress-induced changes in wistar rats *Journal of Stress Physiology & Biochemistry* **9** 136–47 (http://jspb.ru/issues/2013/N1/JSPB_2013_1_136-147.pdf)
[35] Ratheesh M and Helen A 2007 Anti-inflammatory activity of *Ruta graveolens* Linn on carrageenan induced paw edema in wistar male rats *African journal of Biotechnology* **6** 1209–11 (https://ajol.info/index.php/ajb/article/view/57401)
[36] Magaldi S, Mata-Essayag S, De Capriles C H, Perez C, Colella M T, Olaizola C and Ontiveros Y 2004 Well diffusion for antifungal susceptibility testing *International journal of infectious diseases* **8** 39–45
[37] Valgas C, Souza S M D, Smânia E F and Smânia A Jr 2007 Screening methods to determine antibacterial activity of natural products *Brazilian Journal of Microbiology* **38** 369–80
[38] Raheem D J, Tawfike A F, Abdelmohsen U R, Edrada-Ebel R and Fitzsimmons-Thoss V 2019 Application of metabolomics and molecular networking in investigating the chemical profile and antitrypanosomal activity of British bluebells (*Hyacinthoides non-scripta*) *Sci. Rep.* **9** 2547
[39] Abdelmohsen U, Cheng C, Viegelmann C, Zhang T, Grkovic T, Ahmed S, Quinn R, Hentschel U and Edrada-Ebel R 2014 Dereplication strategies for targeted isolation of new antitrypanosomal actinosporins A and B from a marine sponge associated-Actinokineospora sp. EG49 *Marine drugs* **12** 1220–44
[40] Tawfik N F, Tawfike, Abdo R, Abbott G, Abdelmohsen U, Edrada-Ebel R and Haggag E 2017 Metabolomics and dereplication study of the endophytic fungus *Aspergillus chevelieri* in search of bioactive natural compounds *Journal of Advanced Pharmacy Research* **1** 100–9
[41] O'Boyle N M, Banck M, James C A, Morley C, Vandermeersch T and Hutchison G R 2011 Open Babel: An open chemical toolbox *Journal of cheminformatics* **3** 33
[42] Morris G M, Huey R, Lindstrom W, Sanner M, Belew R, Goodsell D and Olson A 2009 AutoDock4 and AutoDockTools4: Automated docking with selective receptor flexibility *J. Comput. Chem.* **30** 2785–91
[43] Taha Z K, Hawar S N and Sulaiman G M 2019 Extracellular biosynthesis of silver nanoparticles from *Penicillium italicum* and its antioxidant, antimicrobial and cytotoxicity activities *Biotechnol. Lett* 1–16
[44] Ahmed S and Ikram S 2015 Silver nanoparticles: one pot green synthesis using *Terminalia arjuna* extract for biological application *J Nanomed Nanotechnol* **6** 309
[45] Anandalakshmi K, Venugobal J and Ramasamy V 2016 Characterization of silver nanoparticles by green synthesis method using *Pedalium murex* leaf extract and their antibacterial activity *Applied Nanoscience* **6** 399–408
[46] Sulaiman G M, T. Hussien H I B A and Saleem M M 2015 Biosynthesis of silver nanoparticles synthesized by *Aspergillus flavus* and their antioxidant, antimicrobial and cytotoxicity properties *Bull. Mater. Sci.* **38** 639–44
[47] Al-Shmgani H S, Mohammed W H, Sulaiman G M and Saadoon A H 2017 Biosynthesis of silver nanoparticles from *Catharanthus roseus* leaf extract and assessing their antioxidant, antimicrobial, and wound-healing activities *Artificial cells, nanomedicine, and biotechnology* **45** 1234–40
[48] Chaiittianan R, Chayopas P, Rattanathongkom A, Tippayawat P and Sutthanut K 2016 Anti-obesity potential of corn silks: Relationships of phytochemicals and antioxidation, anti-pre-adipocyte proliferation, anti-adipogenesis, and lipolysis induction *J. Funct. Foods* **23** 497–510
[49] Chaudhary S, Ceska O, Tétu C, Warrington P, Ashwood-Smith M and Poulton G 1986 Oxypeucedanin, a major furocoumarin in parsley *Petroselinum crispum Planta medica* **52** 462–4
[50] Vokk R, Lõugas T, Mets K and Kravets M 2011 Dill (Anethum graveolens L.) and parsley (*Petroselinum crispum* (Mill.) Fuss) from Estonia: seasonal differences in essential oil composition *Agron. Res* **9** 515–20 (https://agronomy.emu.ee/wp-content/uploads/2011/12/p09s222.pdf#abstract-2849)
[51] Peddicord L A 2013 Determination and quantification of surface lipid metabolites in maize silks: A pathway model for surface lipid biosynthesis based on simultaneous profiling of polar and non-polar metabolites *Graduate Theses and Dissertations* (https://pdfs.semanticscholar.org/a2bc/f916098dbab793bb39439002987ba3f)
[52] Attaurrahman P A, Choudhary M, Hasan N and Sener B 1991 Sophazrine, a Novel Quinolizidine Alkaloid from *Sophora griffithii J. Nat. Prod.* **54** 929–35
[53] Rontani J-F, Pinot F, Kandel S and Aubert C 2005 Visible light-induced oxidation of unsaturated components of cutins: a significant process during the senescence of higher plants *Phytochemistry* **66** 313–21
[54] Larqué-Saavedra A 1979 Studies on the effect of prostaglandins on four plant bioassay systems *Zeitschrift für Pflanzenphysiologie* **92** 263–70
[55] Buckingham J, Baggaly K.H., Roberts A.D. and Szabo L.F. 2010 *Dictionary of Alkaloids with CD-ROM* (CRC press) (https://books.google.com.eg/books?id=mynNBQAAQBAJ&pg=PA909&lpg=PA909&dq=Holadienine;+18-Oxo,+14,15-didehydro&source=bl&ots=JKB9jS2fqg&sig=ACfU3U1UX5T1kQsFGnsRvW4Eydqbl9kTvg&hl=en&sa=X&ved=2ahUKEwjR1cKIuZ3nAhXzBGMBHR10BDMQ6AEwAHoECAgQAQ#v=onepage&q=Holadienine%3B%2018-Oxo%2C%2014%2C15-didehydro&f=false)
[56] Goldblatt A, Hootele C and Pecher J 1970 The alkaloids of *Voacanga thouarsii* var. obtusa *Phytochemistry* **9** 1293–8
[57] Goutarel M, Janot M M, Mathys F and Prelog V 1956 Über das ibolutein *Helv. Chim. Acta* **39** 742–8
[58] Sanchez V, Ahond A, Guilhem J, Poupat C and Potier P 1987 Alcaloides des feuilles de *Didymeles madagascariensis* Willd., des feuilles et des ecorces de racines de Didymeles perrieri Leandri (Didymelacees) *Bulletin de la Société chimique de France* **5** 877–84 (https://searchworks.stanford.edu/view/396266)
[59] Rafsanjany N, Sendker J, Lechtenberg M, Petereit F, Scharf B and Hensel A 2015 Traditionally used medicinal plants against uncomplicated urinary tract infections: are unusual, flavan-4-ol-and derhamnosylmaysin derivatives responsible for the antiadhesive activity of extracts obtained from stigmata of *Zea mays* L. against uropathogenic *E. coli* and Benzethonium chloride as frequent contaminant faking potential antibacterial activities? *Fitoterapia* **105** 246–53
[60] Pérez-Castorena A-L, Martínez-Vásquez M and de Vivar A R 1997 Diterpenes of *Bahia glandulosa Phytochemistry* **46** 729–34
[61] Akak C M, Djama C M, Nkengfack A E, Tu P-F and Lei L-D 2010 New coumarin glycosides from the leaves of *Diospyros crassiflora* (Hiern) *Fitoterapia* **81** 873–7
[62] Hassan G S, Rahman D E A, Abdelmajeed E A, Refaey R H, Salem M A and Nissan Y M 2019 New pyrazole derivatives: Synthesis, anti-inflammatory activity, cycloxygenase inhibition assay and evaluation of mPGES *Eur. J. Med. Chem.* **171** 332–42